MCB
Journals.ASM.org

Reactive Oxygen Species and Epidermal Growth Factor Are Antagonistic Cues Controlling SHP-2 Dimerization

Aurelio Pio Nardozza,[a] Melania D'Orazio,[b] Riccardo Trapannone,[a] Salvatore Corallino,[a] Giuseppe Filomeni,[a,b] Marco Tartaglia,[c] Andrea Battistoni,[a] Gianni Cesareni,[a,d] and Luisa Castagnoli[a]

Department of Biology, University of Rome Tor Vergata, Rome, Italy[a]; IRCCS San Raffaele La Pisana, Rome, Italy[b]; Department of Hematology, Oncology and Molecular Medicine, Istituto Superiore di Sanità, Rome, Italy[c]; and IRCCS Fondazione Santa Lucia, Rome, Italy[d]

The SHP-2 tyrosine phosphatase plays key regulatory roles in the modulation of the cell response to growth factors and cytokines. Over the past decade, the integration of genetic, biochemical, and structural data has helped in interpreting the pathological consequences of altered SHP-2 function. Using complementary approaches, we provide evidence here that endogenous SHP-2 can dimerize through the formation of disulfide bonds that may also involve the catalytic cysteine. We show that the fraction of dimeric SHP-2 is modulated by growth factor stimulation and by the cell redox state. Comparison of the phosphatase activities of the monomeric self-inhibited and dimeric forms indicated that the latter is 3-fold less active, thus pointing to the dimerization process as an additional mechanism for controlling SHP-2 activity. Remarkably, dimers formed by different SHP-2 mutants displaying diverse biochemical properties were found to respond differently to epidermal growth factor (EGF) stimulation. Although this differential behavior cannot be rationalized mechanistically yet, these findings suggest a possible regulatory role of dimerization in SHP-2 function.

SHP-2 is a ubiquitously expressed nontransmembrane protein tyrosine phosphatase (PTP) modulating the cell response to growth factors and cytokines (29). Numerous lines of evidence indicate that this phosphatase promotes the activation of growth pathways and that mutations altering its activity cause congenital or somatic pathologies, such as Noonan and LEOPARD syndromes or leukemia (46, 47). SHP-2 has a simple domain structure in which the enzymatic PTP domain is flanked at the amino-terminal side by two SH2 domains and at the carboxy-terminal side by a relatively unstructured region of approximately 70 residues containing a notable proline-rich motif and a few tyrosine residues that were found to be phosphorylated in phosphoproteomic studies (18, 49). Somewhat contradicting the popular model that phosphatases play a negative role in controlling hormone-dependent signal transduction, SHP-2 is one of the rare tyrosine phosphatases which reinforces activation signals rather than dampening them (37, 42, 52). In the absence of growth factors, SHP-2 has a low basal catalytic activity, whereas it is rapidly activated after growth factor addition to the culture medium (7, 15). A combination of genetic and structural studies have permitted elaboration of an elegant molecular model to explain the pathological consequences of a large number of mutations that are predicted to affect the conformation of the phosphatase (19, 24, 45). The crystallographic structure of SHP-2 shows that the amino-terminal SH2 domain makes extensive contacts with the phosphatase substrate pocket, thus offering a molecular explanation for its low basal activity (15). This model is supported by the observation that the majority of activating mutations causing either the Noonan syndrome or leukemia weaken the interaction between the SH2 and phosphatase domains, thus causing exposure of the phosphatase active site and, as a consequence, relieving its inhibition (45). Under physiological conditions, activation can be achieved by diverting the amino-terminal SH2 domain via an interaction with tyrosine motifs that are phosphorylated upon receptor tyrosine kinase activation (8, 15). In considering alternative modulation mechanisms, we examined the possibility that SHP-2 activity could be regulated by dimerization, similar to that of other members of the tyrosine phosphatase family, such as PTPα, CD45, DEP1, and SAP1 (9, 10, 25, 48). This hypothesis takes roots from at least three different observations: (i) some fragments of SHP-2 aggregate *in vivo* (17); (ii) SHP-1, a close relative of SHP-2, forms homodimers promoting autotransdephosphorylation in living cells (33); and (iii) SHP-1 requires heterodimerization with SHP-2 for correct binding to GRB2-associated binding protein 1 (GAB1) and for activation of the downstream signaling cascade (51).

Here we show that SHP-2 dimerizes in unstimulated cells and that this conformation results in a decrease of catalytic activity. Moreover, we provide evidence that the reversible switch from dimer to monomer is regulated oppositely by reactive oxygen species (ROS) and growth factors, thereby suggesting an alternative redox regulation of SHP-2 structure and activity.

MATERIALS AND METHODS

Reagents and plasmids. The growth factor epidermal growth factor (EGF) was purchased from Upstate Biotechnology. The antibiotics hygromycin B and blasticidin were purchased from Invitrogen, while doxycycline for SHP-2 expression was obtained from BD Transduction Laboratories. A monoclonal antibody for SHP-2 was purchased from BD Transduction Laboratories, polyclonal antibodies for extracellular signal-regulated kinase (ERK) and phospho-ERK were purchased from Cell Signaling, monoclonal antiphosphotyrosine antibody (4G10) and anti-glyceraldehyde-3-phosphate dehydrogenase (anti-GAPDH) were purchased from Upstate Biotechnology, and polyclonal anti-FLAG antibodies

Received 7 December 2011 Returned for modification 3 January 2012
Accepted 24 February 2012
Published ahead of print 12 March 2012
Address correspondence to Gianni Cesareni, cesareni@uniroma2.it, or Luisa Castagnoli, castagnoli@uniroma2.it.

doi:10.1128/MCB.06674-11

were purchased from Sigma-Aldrich. Anti-peroxiredoxin-SO_3 and anti-2Cys-peroxiredoxin antibodies were purchased from Abcam. Anti-rabbit (diluted 1:5,000 in Western blots) and anti-mouse (diluted 1:2,500 in Western blots) secondary antibodies were purchased from Jackson ImmunoResearch. Protein G Sepharose beads and M2 resin used for immunoprecipitations were obtained from Sigma. The 4G10 positive-control antibody was derived from an EGF-stimulated A431 cell lysate (Upstate).

Poly-His-V5-tagged PTPN11 cDNAs (pcDNA6 vector) (SHP-2_V5) and poly-His-tagged PTPN11 cDNAs (pET-26b vector) coding for wild-type SHP2 or mutants carrying the amino acid changes Arg32Gly/Arg138Gly, Thr468Met, Glu76Lys, or Cys333Ser/Cys367Ser/Cys459Ser (SHP-$2^{3C/S}$_V5) were obtained by site-directed mutagenesis (Stratagene).

Generation of stable cell lines expressing FLAG-tagged wild-type SHP-2 and SHP-2^{C459S} mutant. We generated stable cell lines expressing the wild-type and mutant C459S forms of FLAG-tagged SHP-2 in an inducible manner. The HEK293 cell line stably transfected with the pcDNA6/TR regulatory vector (Invitrogen) was transfected with 10 μg of the pcDNA5 FRT/TO vector, encoding SHP-2_FLAG wild-type phosphatase (T-REx-SHP-2 293 cells) or SHP-2^{C459S}_FLAG (T-REx-SHP-2^{C459S} 293 cells), together with 10 μg of the pOG44 (Invitrogen) vector. Lipofectamine 2000 (Invitrogen) was employed as a transfection reagent. Two days after transfection, cells were selected in hygromycin-containing medium (100 μg/ml) for 2 to 3 weeks. The doxycycline-inducible expression of the construct was verified individually for all of the isolated positive clones by adding doxycycline to the medium at a concentration of 2 μg/ml and analyzing the consequent expression by Western blotting.

Cell culture, transfection, *N*-acetyl-L-cysteine (NAC) preincubation, and EGF and H_2O_2 stimulation. HEK293 T-REx cells were cultured and lysed as described previously (11). HEK293 T-REx cells were transfected with Lipofectamine 2000 according to the manufacturer's protocol. After 16 h of starvation in serum- and nutrient-free medium, cells were incubated with 2 μg/ml doxycycline for 6 h (BD Biosciences) and stimulated with 100 ng/ml EGF (Invitrogen) or with 1 mM H_2O_2 (Sigma). Immunoprecipitation and immunoblotting were performed as described previously (11). In the indicated case, the immunoprecipitated proteins were eluted from the beads by twice adding 1.5 ml of 3× FLAG peptide (150 ng/μl) (Sigma) for 30 min at 4°C.

NAC (Sigma) was dissolved in water and pH adjusted to a physiological value (pH 7.0). NAC was then sterilized by filtration before addition to the cell culture. A 10 mM NAC solution was added to the cell culture together with the starvation medium (early balance salt solution [EBSS]; Sigma).

The heterodimer-homodimer complex was prepared as described previously (34).

SHP-2 expression and purification. Recombinant SHP-2 protein was expressed in *Escherichia coli* Rosetta 2(DE3) (Novagen). After 2 h of induction with isopropyl-β-D-thiogalactopyranoside (IPTG; 0.1 mM) at 30°C, the protein was purified by immobilized-metal affinity chromatography, using Ni-nitrilotriacetic acid (Ni-NTA) resin (Qiagen).

Glutathione *S*-transferase (GST) fusion proteins were expressed in *E. coli* BL21. The protein expression was optimized by growing bacteria at 30°C for 4 h after the addition of IPTG to a final concentration of 100 μM. Pelleted bacteria were resuspended in lysis buffer (50 mM Tris, pH 8.0, 5 mM EDTA, 0.1% Triton X-100, 150 mM NaCl) supplemented with a 250 μM proteinase inhibitor mixture (Roche Applied Science) and lysed by treatment with lysozyme (final concentration, 200 μg/ml) for 1 h on ice followed by three rounds of sonication. The lysates were clarified by spinning at 14,000 rpm for 20 min and were bound to glutathione-Sepharose beads (Amersham Biosciences) at 4°C for 1 h. The amount, purity, and integrity of recombinant proteins were evaluated using a protein assay kit (Bio-Rad) and Coomassie blue staining.

Gel filtration chromatography. Two milligrams of 293 T-REx cell lysate was injected onto a Superose 6HR 10/30 fast protein liquid chromatography gel filtration column (GE Healthcare), equilibrated with 50 mM Tris-HCl (pH 7.5), 150 mM NaCl, 1% sodium deoxycholate, 1 mM EDTA, and 1% NP-40, and eluted at a flow rate of 0.25 ml/min with the same buffer. Proteins were collected in 500-μl fractions, precipitated with 10% trichloroacetic acid (TCA), and resolved by SDS-PAGE for immunoblotting.

One milligram of purified SHP-2 recombinant protein was injected onto a Superdex 200HR 10/30 fast protein liquid chromatography gel filtration column (GE Healthcare), equilibrated with 150 mM NaCl, 10 mM HEPES (pH 7.5), eluted at a flow rate of 0.25 ml/min with the same buffer, and collected in 500-μl fractions. Protein fractions were split into 250-μl aliquots that were used for pNPP phosphatase assays and immunoblot analyses.

Gel filtration columns were calibrated with the following molecular mass markers: thyroglobulin (669 kDa), apoferritin (443 kDa), β-amylase (200 kDa), alcohol dehydrogenase (150 kDa), bovine serum albumin (66 kDa), and carbonic anhydrase (29 kDa) (Sigma).

Phosphatase assay. Phosphatase assays of gel filtration fractions were performed by mixing 100 μl of each fraction with 100 μl of PTP buffer (25 mM HEPES, pH 7.4; 50 mM NaCl; 2.5 mM EDTA) and 20 mM pNPP (Sigma) for 30 min at 30°C either under basal conditions or in the presence of 50 μM biphosphotyrosyl protein tyrosine phosphatase non-receptor-type substrate 1 (PTPNS1) (Primm). pNPP dephosphorylation was evaluated by measuring the absorbance at 410 nm.

SPOT synthesis. SPOT synthesis technology (14) was used to synthesize a panel of 51 13-mer peptides corresponding to all the tyrosine residues present in SHP-2, in their nonphosphorylated and phosphorylated forms, on a cellulose membrane (43). Membranes were incubated with the SHP-$2^{N\text{-}SH2/C\text{-}SH2}$ and $GRB2^{SH2}$ domains expressed as GST fusion proteins. The binding efficiency and affinity were revealed using an anti-GST antibody conjugated to horseradish peroxidase. Signal intensity was quantified and plotted in arbitrary units. Positive- and negative-control peptides were also synthesized (7, 41).

RESULTS

SHP-2 forms multimers *in vivo*. We expressed a tetracycline-regulated SHP-2_FLAG protein together with a transfected SHP-2 protein tagged with the V5 epitope to investigate whether SHP-2 forms multimeric aggregates *in vivo*. Figure 1A, lane 2, shows that upon nutrient deprivation, the two proteins coimmunoprecipitated when SHP-2 was not phosphorylated (Fig. 1B), suggesting the formation of multimeric complexes under these experimental conditions. We next checked whether the formation of the SHP-2 complex required an interaction mediated by the SH2 domains of SHP-2. To this end, we performed the same experiment but transfected cells with an SHP-2 mutant containing two R-to-G substitutions, at positions 32 and 138 in the SH2 domains (SHP-2_V5-RR), which convert the essential FLVRES motifs of the tandem SH2 domains into FLVGES. This double mutation impairs the capability of SH2 domains to bind phosphotyrosine peptides *in vitro* (39). In starved cells, the SHP-2_V5-RR mutant coassociated with the SHP-2_FLAG phosphatase as efficiently as the wild-type protein did (Fig. 1A, lane 3), suggesting that the SH2 domain has no role in SHP-2 self-association. In addition, we verified by SPOT analysis whether the SH2 domains of SHP-2 could bind efficiently to the phosphorylated forms of any of the 23 tyrosine residues in the SHP-2 sequence. The membranes were probed with the tandem SH2 domains of SHP-2 (SHP-$2^{N\text{-}SH2/C\text{-}SH2}$). As a positive control, the same peptides were also probed with the SH2 domain of the GRB2 adaptor protein, known to interact with the phosphorylated Tyr_{584} residue of SHP-2 (50). Figure 1C shows that aside from the positive controls, no phosphotyrosine-containing peptide was able to significantly bind the SHP-$2^{N\text{-}SH2/C\text{-}SH2}$ domains, with the exception of p-Tyr_{525}. However, this residue was never

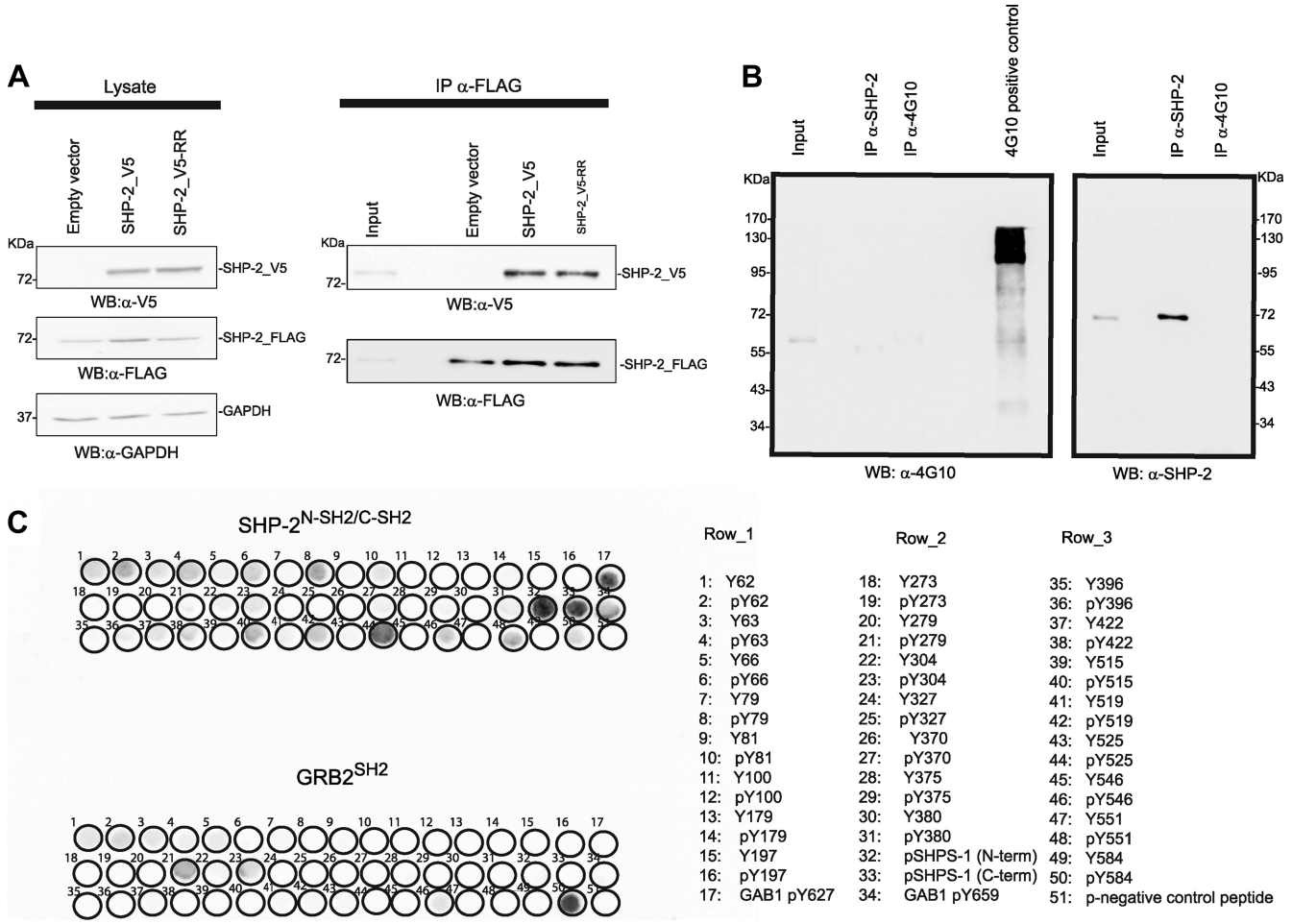

FIG 1 SHP-2 forms multimeric complexes in resting cells, and this homo-association is not dependent on functionally active SH2 domains. (A) T-REx SHP-2 293 cells were transfected with SHP-2_V5 phosphatase, the double arginine mutant SHP-2_V5-RR, or an empty vector as a control. The transfection efficiency of SHP-2_V5 and SHP-2_V5-RR was monitored by immunoblotting (WB) with anti-V5 antibody (α-V5), while the induced expression of SHP-2 FLAG was visualized with anti-FLAG antibody (α-FLAG). Equal gel loading was assessed with anti-GAPDH antibody (α-GAPDH). Whole-protein extracts were immunoprecipitated (IP) with anti-FLAG antibody, and the presence of coimmunoprecipitated SHP-2_V5 was detected with anti-V5 antibody. Immunoprecipitation was checked with anti-FLAG antibody. Immunoblots are from one experiment representative of three that gave similar results. (B) T-Rex SHP-2 293 cells were starved for 16 h and then lysed. The whole-protein extract was immunoprecipitated with anti-SHP-2 antibody (α-SHP-2) and with an anti-p-Tyr antibody (α-4G10). Proteins were revealed with both anti-SHP-2 and anti-4G10 antibodies. (C) All 51 peptides containing a tyrosine residue in the SHP-2 phosphatase were synthesized on cellulose membranes, each in unphosphorylated and tyrosine-phosphorylated versions, together with control peptides (as reported in the list). The membranes were probed with the tandem SH2 domains of SHP-2 (SHP-$2^{N\text{-}SH2/C\text{-}SH2}$) or, as a control, with the SH2 domain of GRB2 (GRB2^{SH2}), both expressed as GST fusion proteins. Binding of the SH2 domains to the immobilized peptides was revealed using an anti-GST antibody conjugated to a fluorophore.

found phosphorylated under any physiological or pathological conditions (16). Taken together, these data indicate that SHP-2 is able to self-associate in cells and that this association is not mediated by interactions between the SH2 domains and phosphotyrosine peptides.

SHP-2 exists both as a dimer and as a monomer in resting cells. To further investigate the biochemical nature of SHP-2 self-association, we purified SHP-2 complexes by means of the strategy shown in Fig. 2A. This approach is based on the coexpression of SHP-2 proteins fused to two different tags (FLAG and His-V5) followed by two sequential immunoprecipitations to isolate complexes that bind antibodies against both tags. To provide evidence of a 1:1 molar ratio in the purified protein complex, we started with unequal stoichiometric levels of FLAG-tagged versus His-V5-tagged SHP-2 proteins (Fig. 2B, lane 3). In the first affinity purification step, SHP-2_FLAG was immunoprecipitated with an anti-FLAG antibody and then eluted with an excess of the FLAG peptide (Fig. 2B, lane 1) to yield SHP-2_FLAG monomers and multimers. The eluted sample was further immunoprecipitated with anti-His antibodies to obtain only SHP-2 complexes containing FLAG-tagged together with His-tagged monomers. The observation that FLAG- and His-tagged SHP-2 molecules were present in equivalent amounts in the immunopurified complex, despite their stoichiometric difference in the cell, is consistent with the hypothesis that the aggregated forms of SHP-2 consist mostly of dimers (Fig. 2B, lane 2).

Endogenous SHP-2 forms homodimers *in vivo*. To gain better insights into the nature of the SHP-2 dimeric interaction, we estimated the molecular masses of SHP-2 aggregates by gel filtration chromatography. Cell lysates prepared from starved HEK293 cells were loaded onto a Superose 6HR 10/30 column, and fractions were collected. Immunoblot analysis with anti-SHP-2 antibody revealed that SHP-2 was enriched in two fractions, with es-

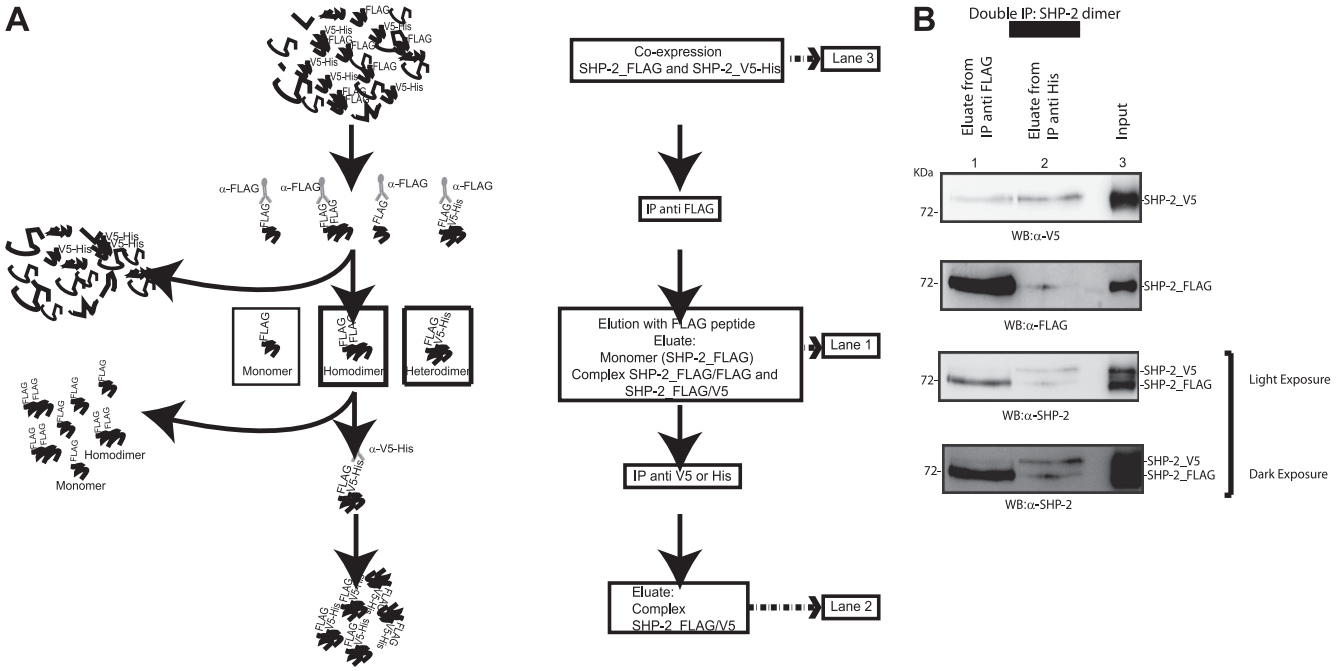

FIG 2 SHP-2_V5–SHP-2_FLAG complex. (A) Graphical view and experimental procedure for isolation of the SHP-2_V5–SHP-2_FLAG complex. (B) T-REx SHP-2 293 cells were transfected with a plasmid encoding SHP-2_V5. The expression of FLAG-tagged SHP-2 was induced with doxycycline for 12 h. Cells were starved and then lysed. The heterodimeric SHP-2 complex was isolated as described in panel A and in Materials and Methods. The levels of SHP-2_V5 and SHP-2_FLAG proteins in each step of sequential immunoprecipitations were verified by Western blotting with anti-V5, anti-FLAG, and anti-SHP-2 antibodies. Lane 2 was loaded with 2.5 times the amount loaded in lane 1. This step of immunoprecipitation was repeated three times independently.

timated molecular masses of about 60 and 120 kDa, in good agreement with the calculated masses of monomeric and dimeric SHP-2, respectively (Fig. 3). These data further support the existence of a dimeric form of endogenous SHP-2 in resting cells. Moreover, densitometric analyses of band intensities were consistent with approximately 15% of SHP-2 existing as a stable dimer under these conditions.

SHP-2 dimers are stabilized by disulfide bonds. Once we excluded the possibility that SHP-2 dimerization is driven by a phospho-Tyr–SH2 domain interaction, we asked whether the dimerization might be regulated by disulfide bonds, which is a common mechanism to promote and regulate protein self-association (3, 21, 27). To address this question, an aliquot of coimmunoprecipitated SHP-2_FLAG and SHP-2_V5 was subjected to nonreducing SDS-PAGE followed by immunoblot analysis. Figure 4A, lane 2, shows that under these conditions, a 130-kDa band, consistent with the dimeric form of SHP-2, was recognized by the anti-V5 antibody. Interestingly, this band was not observed when the sample was treated with dithiothreitol (DTT), while a new band, comigrating with the monomeric form of SHP-2, appeared. These results confirm that multimeric SHP-2 is a homodimer which is held together by disulfide bonds. In a parallel experiment, we pretreated an aliquot of the cell extract with DTT before immunoprecipitation to disrupt any complex mediated by disulfide bridges. This pretreatment completely abolished the ability of SHP-2 to self-associate in a dimeric complex (Fig. 4B).

SHP-2 dimerization is regulated by ROS. Since cells produce ROS under serum and nutrient starvation conditions (Fig. 5C) (36), we further investigated whether the sulfhydryl redox state could be an important player in SHP-2 dimerization. Dimer formation was analyzed in starved cells upon pretreatment with the thiol antioxidant NAC, which replenishes intracellular glutathione, or upon H_2O_2 addition, which gives rise to widespread thiol oxidation. Figure 5A shows that cells pretreated with NAC had a reduced amount of dimeric SHP-2 (approximately 50%), whereas H_2O_2 caused a 3-fold increase in the amount of dimer complex with respect to that in untreated cells. Note that this dramatic increase in dimer content in cells treated with H_2O_2 was also confirmed by an enhancement of the intensity of the 130-kDa band when the immunoprecipitated sample was loaded on an SDS-PAGE gel under nonreducing conditions (Fig. 5B). To confirm that the cell redox state can modulate the monomer-dimer equilibrium of endogenous SHP-2, we used gel filtration chromatography to analyze the change in oligomerization state of SHP-2 when the cells were treated with H_2O_2. As shown in Fig. 5C, dimeric SHP-2 was more abundant (about 2.5 times) in cells treated with H_2O_2, suggesting that the monomeric-dimeric SHP-2 equilibrium is influenced by the cellular redox state.

SHP-2 dimerization is accompanied by a decrease in PTPase activity. In order to investigate whether dimerization could affect phosphatase activity, recombinant SHP-2 was expressed in *E. coli*, and after gel filtration, protein activities of the fractions enriched in dimers (fractions 53 to 56) and monomers (fractions 59 to 61) were measured. We determined the basal activity as well as the activity following stimulation with the biphosphorylated target PTPNS1, a peptide able to convert a closed and inactive monomeric SHP-2 molecule into an open and active molecule (23, 31). Figure 6 shows that the phosphatase activity of the dimeric fraction was approximately three times lower than that of the monomer, supporting the notion that SHP-2 dimerization is associated

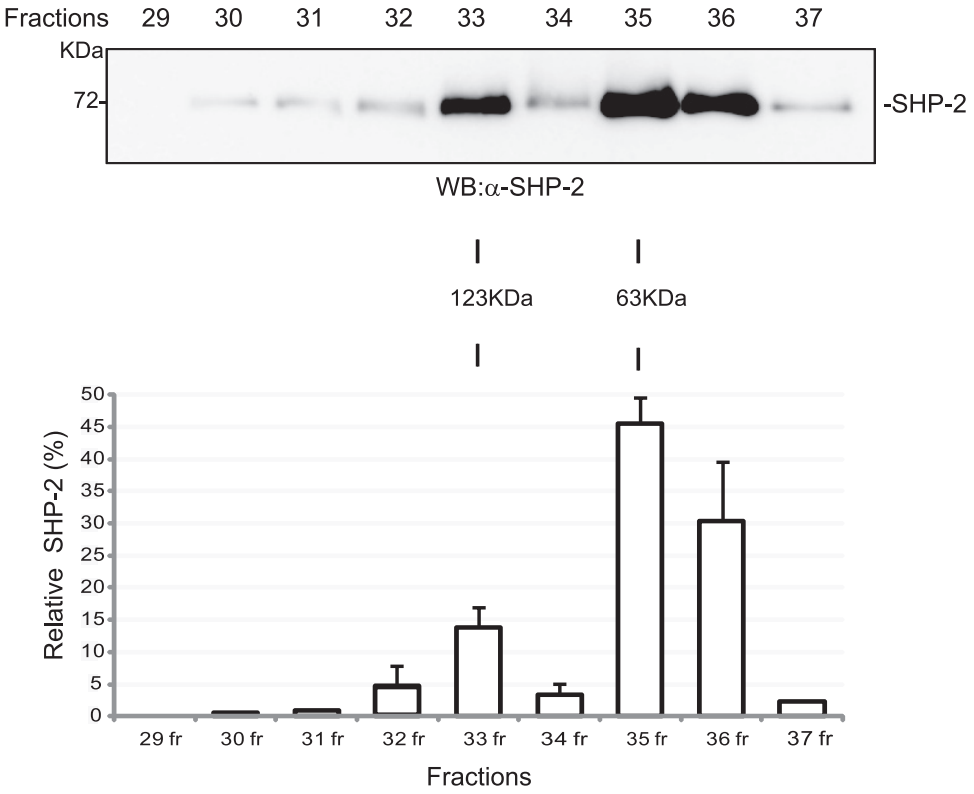

FIG 3 Endogenous SHP-2 forms dimers in resting cells. HEK293 cells were starved in EBSS medium, lysed, and subjected to gel filtration. (A) Fractions 29 to 37 were precipitated with TCA, separated by SDS-PAGE, and then immunoblotted with anti-SHP-2 antibody. Estimated molecular masses were calculated from the standard curve produced from the gel filtration molecular size markers. (B) Densitometric scanning (Aida software) results for the Western blot in panel A.

with a significant decrease in its activity. Furthermore, the binding of the SH2 domains entangled in the dimer to the tyrosine-phosphorylated peptide was not sufficient to convert the dimer into fully activated monomers, at least *in vitro*.

Mutation of the catalytic cysteine partially impairs SHP-2's dimerization ability. Many protein tyrosine phosphatases have a redox-sensitive cysteine at the catalytic site. Since we observed that the catalytic activity of the dimer was lower than that of the monomer and we showed that SHP-2 dimerization was influenced by the cellular redox state, we asked whether the catalytic cysteine could be involved in this process. To this end, we engineered a stable HEK293 cell line expressing an SHP-2_FLAG phosphatase in which the catalytic cysteine was replaced with a serine (T-REx-SHP-2^{C459S} 293 cells). This mutant was catalytically inactive but

FIG 4 SHP-2 dimerization is mediated by a disulfide bridge. T-Rex SHP-2 293 cells were transfected with SHP-2_V5 phosphatase, and expression of SHP-2_FLAG was induced for 6 h with doxycycline. The SHP-2_FLAG protein and its molecular partners were immunoprecipitated with anti-FLAG antibody and then treated with DTT. The asterisk indicates a band with an M_r of about 130,000 that was visible only when DTT was omitted in the loading dye. Immunoblots are from one experiment representative of three that gave similar results. (B) T-Rex SHP-2 293 cells were transfected with SHP-2_V5 phosphatase induced with doxycycline. The lysate was split in two, and one half was treated with DTT for 15 min (lane 2). The SHP-2_FLAG protein was immunoprecipitated, and the interaction was revealed by probing with anti-V5 antibody.

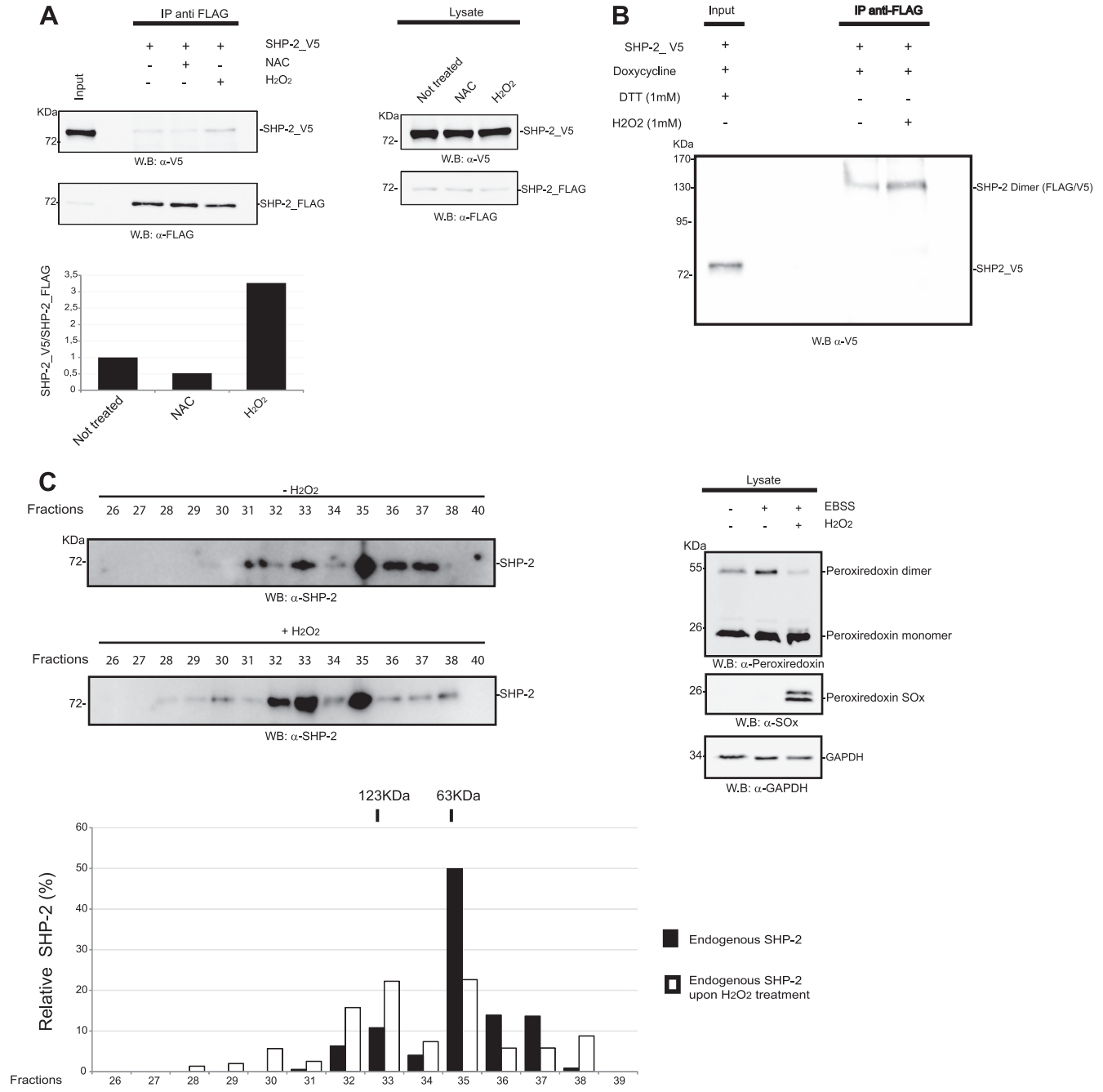

FIG 5 The amount of SHP-2 dimer is regulated by ROS. (A) Hydrogen peroxide increases the dimeric fraction. T-REx SHP-2 293 cells were transfected with SHP-2_V5 and induced with doxycycline to allow the expression of the SHP-2_FLAG phosphatase. Before starvation, 1/3 of the culture was incubated with 10 mM NAC. Cells were starved, and 1 h before lysis, one of the two untreated samples was incubated with 1 mM H_2O_2. Cells were lysed, and the SHP-2_FLAG phosphatase and its interactors were immunoprecipitated with anti-FLAG antibody. The presence of the SHP-2_V5 interactor partner was verified by probing the immunoprecipitate-containing resolved SDS-PAGE gel with anti-V5 antibody. Proper immunoprecipitation was assessed by blotting with anti-FLAG antibody. The ratio of V5 to FLAG was quantified and plotted in the bar chart. The expression of SHP2_FLAG and SHP-2_V5 in the lysates is shown. (B) T-Rex SHP-2 293 cells were transfected with SHP-2_V5 phosphatase, and expression of SHP-2_FLAG was induced for 6 h with doxycycline. Before lysis, one sample was treated with 1 mM H_2O_2. The SHP-2_FLAG protein and its binding partners were immunoprecipitated with anti-FLAG antibody, and then the immunoprecipitates were analyzed by SDS-PAGE without the addition of DTT in order to detect the dimeric form. (C) 293 cells were starved in serum- and nutrient-free medium and then either lysed or treated with 1 mM H_2O_2 and then lysed. The lysate was applied onto a Superose 6HR 10/30 gel filtration column. Fractions 26 to 40 were precipitated with TCA, separated by SDS-PAGE, and then immunoblotted with anti-SHP-2 antibody. Estimated molecular masses were calculated from the standard curve produced with the gel filtration molecular size markers described in Materials and Methods. Densitometric scanning results for the Western blot in panel C are also reported. The measurement of the cellular redox state was assessed by Western blotting with anti-peroxiredoxin-SO_3 and anti-2Cys-peroxiredoxin antibodies.

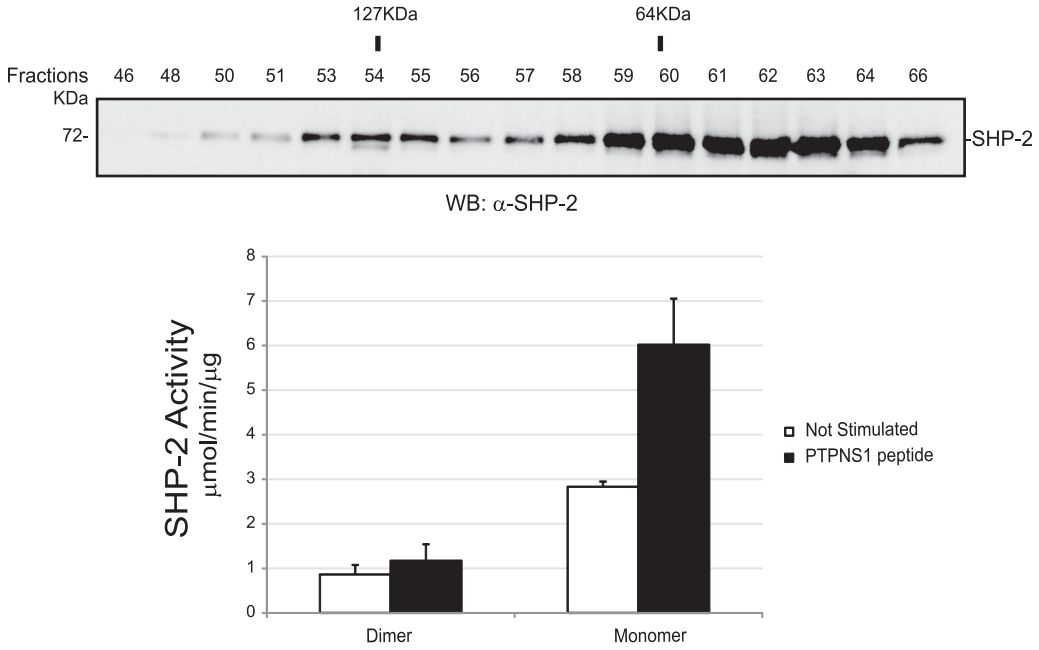

FIG 6 The dimer has a specific catalytic activity that is 3-fold lower than that of the monomer. The SHP-2 recombinant protein was expressed in *E. coli* and purified as described in Materials and Methods. Five hundred micrograms of SHP-2 was loaded onto a Superdex 200HR 10/30 column. (Top) An aliquot of the proteins from each fraction (fractions 46 to 66) was precipitated with TCA, separated by SDS-PAGE, and immunoblotted with anti-SHP-2 antibody. (Bottom) Bar graph representation of the mean specific activities (expressed as μmol/min/μg) toward pNPP of the fractions enriched in SHP-2 dimers (fractions 53 to 56) and the fractions enriched in monomers (fractions 59 to 62), without (white bars) and with (black bars) stimulation with biphosphorylated PTPNS1 peptide. The molecular size of proteins eluted in each fraction was estimated based on the standard curve derived from the molecular size markers after migration in a Superdex 200HR 10/30 column.

retained the ability to correctly localize and bind to substrates (data not shown) (2). Figure 7A shows that the amount of the SHP-2^{C459S}/SHP-2^{wt} dimer was reduced to approximately 60% of the wild-type dimer level, suggesting that the catalytic cysteine contributes to modulating dimer formation, without being required. We further mutagenized the two backdoor cysteines (C333 and C367) that are nearest (9 to 12 Å) to the catalytic residue and have been described as forming disulfide bonds in order to protect the enzyme from irreversible oxidation (6). The triple SHP-2 mutant SHP-$2^{3C/S}$_V5 showed only a moderate decrease in the percentage of dimeric phosphatase, suggesting that the backdoor cysteines have hardly any effect on dimerization (Fig. 7B).

The amount of SHP-2 dimers correlates inversely with activation of the Ras/mitogen-activated protein kinase (MAPK) pathway. SHP-2 is an acknowledged activator of the EGF and other signal transduction pathways. Since the experiments described so far were performed in starved cells, and since EGF stimulation is not associated with ROS generation (26), we next asked whether the assembly of the dimeric complex was dynamically influenced by stimulation with epidermal growth factor. Cells were treated with EGF, and dimer formation was monitored after 5 and 60 min. After 5 min, the activation of ERK1/2 reached its maximum, while at 60 min it returned to the basal level (Fig. 8A) (32, 37). As shown in Fig. 8B, the amount of SHP-2 dimer was halved after 5 min of EGF treatment, while it was restored after 60 min. These findings indicate that SHP-2 dimerization is reversible and is modulated by the pathway activated by EGF. Moreover, dimerization correlated inversely with the activation level of ERK1/2, suggesting a possible role for SHP-2 dimerization in the modulation of receptor tyrosine kinase pathways.

We have already shown that the SHP-2 SH2 domains, or at least their ability to bind phosphopeptides, are not involved in modulating phosphatase dimerization under resting conditions. Since the activation of SHP-2 requires phosphorylation of tyrosines in the target proteins, we next asked whether R32G and R138G mutations in the SH2 domains could influence dimer disassembly after stimulation with growth factors (Fig. 8C). While the relative amount of the wild-type dimer decreased to approximately 50% after 5 min of EGF induction, the dimer with the mutant SHP-2_V5-RR protomer did not dissociate appreciably, implying that the resolution of the SHP-2 dimer after EGF induction requires functional SH2 domains in both protomers.

Different mutants of SHP-2 show different dimerization profiles. Mutations in the SHP-2 protein cause pathogenic conditions associated with dysregulation of Ras signaling. We investigated whether pathological SHP-2 mutants could dimerize with wild-type SHP-2 when expressed in heterozygosity. The T468M and Y279C mutations are catalytically inactivating mutations causing LEOPARD syndrome (LS), while the E76K mutation is a mutation resulting in a hyperactive phosphatase, implicated in leukemia. Although all of the mutants were able to dimerize with the coexpressed wild-type SHP-2_FLAG protein in unstimulated cells (Fig. 9A), the SHP-2^{T468M}-containing dimer was significantly less abundant. Remarkably, it did not dissociate following EGF stimulation, in contrast to what was observed for wild-type SHP-2 dimers, SHP-2^{E76K}/SHP-2^{wt} dimers (Fig. 9B), and SHP-2^{Y279C}/SHP-2^{wt} dimers (data not shown). As already reported, the ectopic expression of wild-type SHP-2 stimulates the activation of ERK after EGF incubation. A similar stimulation was observed under our conditions after transfection with SHP-2^{T468M}. This

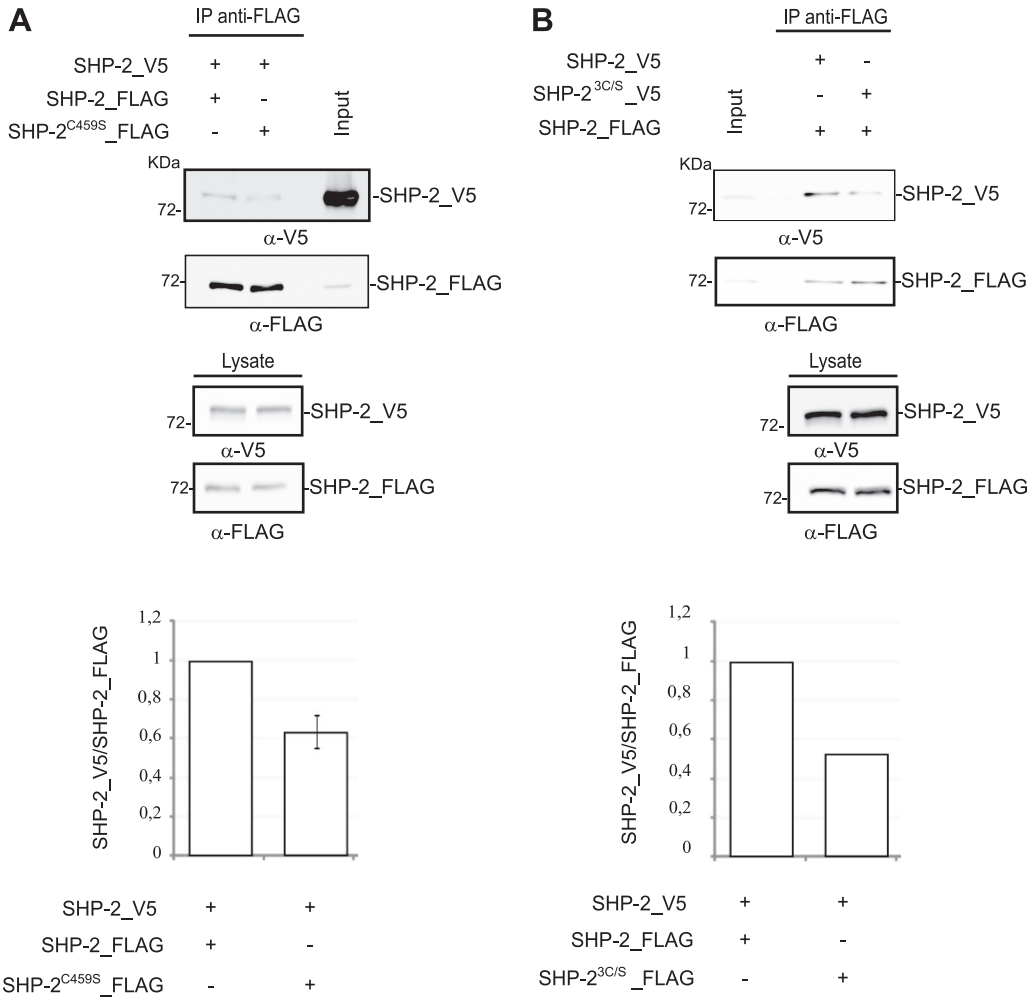

FIG 7 The catalytic cysteine of SHP-2 plays a role in SHP-2 dimerization. T-Rex 293 cells transfected with SHP-2_V5 (A and B) or the SHP-$2^{3C/S}$_V5 mutant (B) were induced to express either the SHP-2_FLAG wild type (A and B) or the C459S mutant (A). The cells were then starved and lysed. The SHP-2_FLAG phosphatases were immunoprecipitated with anti-FLAG antibody, and the interacting SHP-2_V5 protein was revealed with anti-V5 antibody. The input, the control for immunoprecipitation, and the expression of the SHP-$2^{3C/S}$_V5 and SHP-2^{C459S}_FLAG mutants are also shown. The ratios of the quantified intensities of the SHP-2_V5 band and the SHP-2 FLAG band in each experiment are represented in the bar charts at the bottom.

may seem in contradiction with what has been reported by Kontaridis et al. (20). However, note that they performed a comparable experiment, but after ectopic expression of GAB1 and ERK, and that the role of this LEOPARD mutant in the activation of ERK is still controversial (20, 30). SHP-2^{Y279C} is a loss-of-function mutant with an altered side chain of the residue that sets the depth of the catalytic cleft, while the T468 residue is part of the catalytic motif (22). The different dimerization profiles observed for the two LEOPARD mutants could be ascribed to the profound destabilization of the catalytic domain caused by the T468M mutation.

DISCUSSION

Over the past decade, evidence has accumulated that the tyrosine phosphatase SHP-2 can positively modulate signaling events following receptor tyrosine kinase stimulation (38, 42). Different models have been proposed to explain the mechanisms by which this phosphatase enhances signal flow through Ras. According to the most credited one, SHP-2 adopts an inactive conformation in resting cells. Phosphorylation of an SH2 docking site on adaptor proteins (e.g., GAB1) has the dual effect of both activating the phosphatase and directing its activity to dephosphorylate tyrosine residues of target proteins. Among them, receptors and adaptors that constitute docking sites for proteins that negatively control RAS function (e.g., GAPs) or regulatory sites of other signaling repressors (e.g., SPRTYs) have been reported (24, 28). Given this central role, keeping SHP-2 function under control is crucial for cell homeostasis, and mutations leading to uncontrolled SHP-2 activation result in developmental pathologies or cancer (44).

Available crystallographic and biochemical data are consistent with a model whereby, under unstimulated conditions, SHP-2 activity is negatively regulated by intramolecular interactions between residues in the backside loop of the amino-proximal SH2 domain and the catalytic pocket of the PTP domain. The phosphatase is activated by disrupting these autoinhibitory interactions when the phosphotyrosine binding pockets in the SH2 domains are engaged in phosphopeptide binding (5, 15).

Here we provide evidence for a new regulatory mechanism based on SHP-2 dimerization, and we show that this mechanism

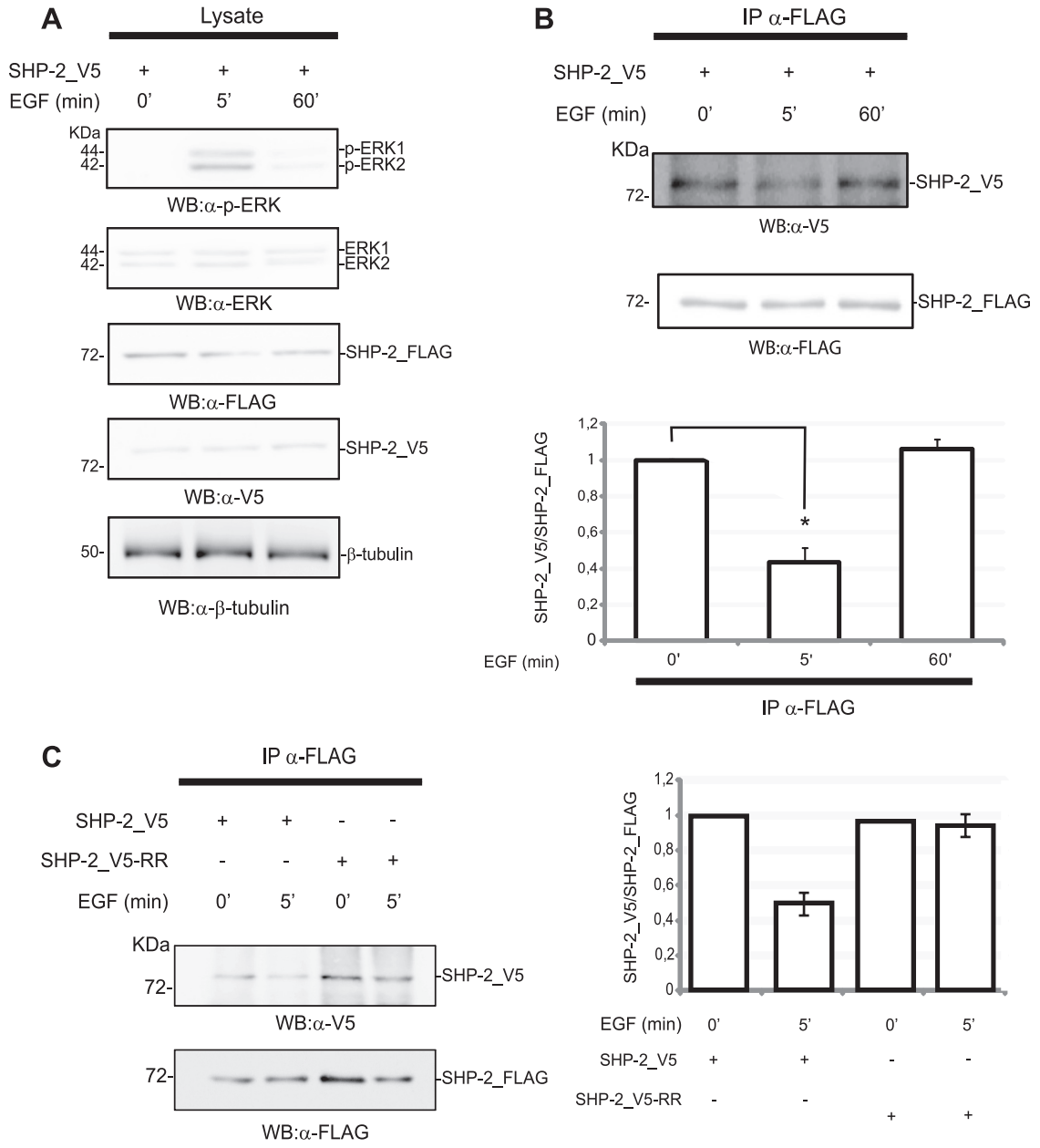

FIG 8 SHP-2 dimerization correlates inversely with MAPK activation upon EGF induction. T-REx SHP-2 293 cells were both transfected with SHP-2_V5 phosphatase and induced with doxycycline to allow the expression of the SHP-2_FLAG phosphatase. The transfected and doxycycline-induced cultures were incubated with EGF (100 ng/ml), and aliquots were sampled at 0, 5, and 60 min. (A) Transfection efficiency and doxycycline induction were assessed by revealing the blot with anti-V5 antibody and anti-FLAG antibody. The activation levels of ERK1/2 proteins were monitored by probing with anti-phopho-ERK1/2 (α-p-ERK) and anti-ERK1/2 (α-ERK) antibodies. Equal gel loading was assessed by probing the β-tubulin levels. (B) At the indicated time, an aliquot of protein extract was immunoprecipitated with anti-FLAG antibody. The amount of coimmunoprecipitating SHP-2_V5 was revealed with anti-V5 antibody. The anti-FLAG immunoprecipitation was confirmed with anti-FLAG antibody. The intensities of the immunoprecipitated bands were quantified and the values plotted in a bar diagram, with 1 considered the maximum amount of SHP-2_V5 coimmunoprecipitated protein. The error bars were calculated for five independent experiments (5 min of EGF induction) (Student's *t* test; $P < 0.001$) or three independent experiments (60 min of EGF induction). (C) Fully functional SH2 domains are required for dimer resolution upon EGF induction. T-Rex SHP-2 293 cells were transfected with SHP-2_V5 and SHP-2_V5-RR. The wild-type FLAG-tagged phosphatase was induced by adding doxycycline to the medium. Cells were starved, induced for 5 min with EGF, and then lysed. The total lysates were immunoprecipitated with anti-FLAG antibody, and the interacting SHP-2_V5 protein was revealed with anti-V5 antibody. The immunoprecipitated bands were quantified, and the ratio of V5 to FLAG is shown in the bar chart, with 1 considered the highest SHP-2_V5/FLAG dimerization level.

can be modulated by the cell redox state. In particular, we have shown that SHP-2 can dimerize *in vivo*, and we suggest that this SHP-2 state represents a new mechanism that contributes to maintaining a stable pool of SHP-2 in an inactive conformation in unstimulated cells.

We demonstrated that at least 15% of SHP-2 in resting cells is in a dimeric form *in vivo*. The dimer/monomer ratio, however, is not static and follows a kinetics that inversely correlates with the activation of the MAPK pathway. After 5 min of incubation with EGF, when ERK activation reaches its maximum, approximately

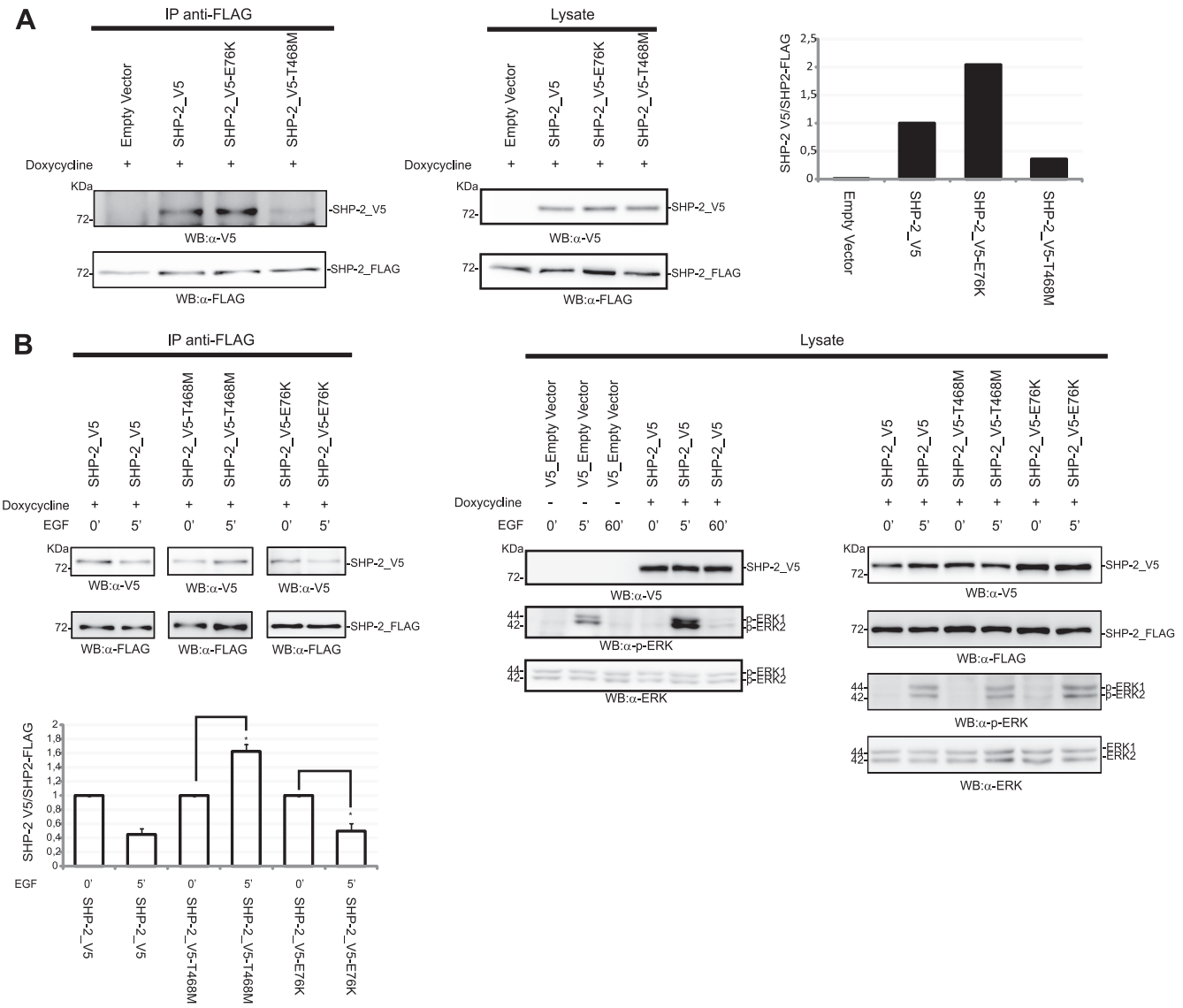

FIG 9 Dimerization of the LEOPARD mutant SHP-2^{T468M} shows altered kinetics upon EGF induction. 293 T-REx cells expressing the wild-type phosphatase SHP-2_FLAG were transfected with SHP-2_V5, the LEOPARD mutant SHP-2_V5-T468M, or the leukemic mutant SHP-2_V5-E76K. Expression of SHP-2_FLAG was induced for 6 h with doxycycline. Cells were starved in serum-free medium for 16 h and then lysed (A) or induced with EGF for 5 min (B). Lysates were immunoprecipitated with anti-FLAG antibody, and coimmunoprecipitated SHP-2 was revealed with anti-V5 antibody. The ratio between the coimmunoprecipitated SHP-2_V5 and the immunoprecipitated SHP-2_FLAG under starvation conditions is visualized in the upper bar chart. The lower bar chart shows the difference of dimeric content upon EGF induction, with 1 considered the level of dimers measured before EGF induction. The transfection efficiency was verified by revealing the PAGE-separated proteins with the anti-V5 antibody. Immunoprecipitation was verified with anti-FLAG antibody. The levels of SHP-2 proteins in the lysates were visualized by Western blotting either with anti-FLAG or with anti-V5. The EGF-induced phosphorylation profile of ERK1/2 proteins was monitored by probing with anti-phospho-ERK1/2 and anti-ERK1/2 antibodies. The error bars were calculated for three independent experiments (Student's *t* test; $P < 0.05$). The EGF time course (0, 5, and 60 min) shown in panel B (lysate panel) was an independent experiment to compare ERK1/2 activation in mock- and SHP-2_V5-transfected cells.

50% of SHP-2 dimers dissociate, to finally restore basal levels when ERK activation tails away. Tyrosine phosphorylation and the ensuing formation of complexes mediated by phosphotyrosine binding domains play a major regulatory role in the activation of growth pathways. Although the amount of SHP-2 dimer in resting cells does not depend upon interactions mediated by its two SH2 domains, dimer resolution following EGF stimulation is affected by mutations influencing the SHP-2 phosphopeptide binding pocket as well as by the oxidative state of the SHP-2 molecule. This evidence suggests that the dimer-monomer equilibrium is modulated by a change in conformation triggered by the interaction of the SH2 domains with a phosphorylated target and that it is affected by the cell redox state (35).

The observation that purified wild-type homodimers expressed in *E. coli* have a 3-fold-decreased activity compared to monomers implies that the modulation of the dynamic dimer-monomer equilibrium is likely to affect the basal level of SHP-2 activity in resting cells. The functional consequences of this observation are unclear, since until now the residual activity of the SHP-2 monomer in the closed conformation has not been linked to any function.

Both "closed" monomers and dimers are converted to fully activated monomers upon binding of the SH2 domains to a phosphorylated target. The relative importance of the two control mechanisms (closed-open and monomer-dimer), as well as whether and how this balance can be altered by mutations, depends on the monomer/dimer ratio in the different cell backgrounds and on the ability to selectively alter either mechanism by specific mutations. Most activating SHP-2 mutations can be explained on the basis of an alteration of the interaction surface between the amino-terminal SH2 domain and the phosphatase catalytic pocket. However, a number of additional mutations still await a convincing molecular interpretation (45).

Our data do not provide much information on the dimer topology; for instance, we do not know whether each subunit of the SHP-2 dimer is in a conformation that is similar to the one observed in the crystal structure or whether dimerization requires a large conformational change. Huang et al. investigated the potential intramolecular interactions in SHP-2 by use of progressive deletions, and they demonstrated that the catalytic domain of the phosphatase is able to interact both with the SH2 domains and with itself (17). Although structural characterization of the dimer is beyond the scope of our work, we cannot exclude a head-to-tail topology, since the intramolecular interaction between the amino-terminal SH2 domain and the phosphatase domain observed in the crystallographic structure could support this hypothesis. However, we deem this unlikely, since the E76K mutant, which has a disrupted inhibitory interaction promoting an open conformation, is still able to dimerize with the wild-type counterpart. Similarly, we can confidently exclude that the dimer relies on intermolecular binding between the SH2 domains and phosphotyrosines in the carboxy-terminal domain. In fact, the double mutant SHP-2_V5_RR, with both SH2 domains inactivated in the phosphotyrosine peptide binding pocket, dimerizes with an efficiency comparable to that of the wild-type protein. Huang et al. (17) suggested that a C-terminal region of SHP-2 (residues 399 to 593) may drive multimerization and that this multimeric assembly is positively modulated by GAB1 expression. However, they also reported that this region, in addition to the SH2 domains, promotes the interaction with GAB1. Although these observations may be relevant to understanding the modulation of the dimer-monomer equilibrium dynamics, they add an extra level of complexity that is difficult to reconcile in a simple model.

Presently, our limited understanding of the dimer topology does not allow the identification of disease mutations that are likely candidates for mutations affecting the dimer-monomer equilibrium. In this respect, an intriguing observation is that the LS-causing T468M mutant expressed together with the wild-type phosphatase not only has a lower capacity to form dimers but also displays an altered dimer resolution kinetics upon growth factor stimulation. Interestingly, the levels of SHP-2^{T468M} heterodimers reached wild-type levels after EGF stimulation. The LS-causing SHP-2^{T468M} mutant causes a decrease in phosphatase activity (20) and is associated with the formation of a more stable complex with GAB1 (13). In addition, this substitution has been predicted to destabilize the closed phosphatase conformation (20). It is likely that this property, either directly or indirectly, affects the ability of this mutant to form and resolve a complex with wild-type SHP-2. Any speculation about the functional consequences that this altered dimer resolution kinetics may have on the regulation of the Ras pathway in heterozygosis is frustrated by the lack of information on the activity of the SHP-2^{T468M}/SHP-2^{wt} heterodimer.

Importantly, our studies demonstrate that the SHP-2 monomer-dimer equilibrium is affected by the cell redox state. A variety of reports have implicated ROS as modulators of signal transduction, either promoting or inactivating a variety of pathways in various cell types (1). Early reports showed that receptor tyrosine kinase activation leads to a transient H_2O_2 production that is required for full tyrosine phosphorylation signaling (40). PTPs, due to the presence of the catalytic cysteine and their predominant negative role in signaling, were first proposed and then demonstrated to be functionally important ROS targets (12). To date, different studies have reported oxidation of specific PTPs, including SHP-2, in platelet-derived growth factor (PDGF) signaling (26). In 2002, Meng and coworkers demonstrated that a PDGF-stimulated production of ROS determines a transient oxidation and inactivation of SHP-2 in Rat-1 fibroblasts (26). Moreover, they demonstrated that the oxidation and inactivation of SHP-2 were induced only by PDGF, not by EGF or fibroblast growth factor (FGF), in accordance with the accepted model that SHP-2 plays a positive role in regulating signaling from the activation of FGF and EGF receptors (4, 35). In our experimental model, we observed that SHP-2 is able to self-associate in a dimeric complex under conditions of growth factor and nutrient depletion, while incubation with EGF promotes dimer dissociation. This is consistent with the observations that dimers are preferentially formed under oxidative conditions and that ROS are produced under starvation conditions (data not shown) (36). In contrast, EGF binding to its receptor, in contrast to the case with PDGF, does not result in ROS generation (26). Dimerization by disulfide bonds could contribute to protecting the catalytic cysteine sulfenic acid from further irreversible oxidation, as an alternative to sulfenylamide formation or intramolecular disulfide bond formation. We measured a reduction of the dimeric state when the catalytic cysteine was mutated to serine. From these data, we conclude that the catalytic cysteine is important for dimerization, though not necessary. In contrast, changing the two highly conserved backdoor cysteines did not have any appreciable extra negative effect on dimerization efficiency. This observation is in agreement with a previous report describing the final oxidized state of SHP-2 as consisting of a novel combination of a reduced catalytic cysteine and a "backdoor disulfide" (6).

ACKNOWLEDGMENTS

We thank Simone Cardaci for help with ROS analysis.

This work was supported by grants from the Italian Association for Cancer Research (AIRC), Telethon (GGP09243), and the European Network of Excellence (ENFIN) to G.C. and by a grant from Telethon (GGP10020) to M.T.

REFERENCES

1. **Adler V, Yin Z, Tew KD, Ronai Z.** 1999. Role of redox potential and reactive oxygen species in stress signaling. Oncogene **18**:6104–6111.
2. **Agazie YM, Hayman MJ.** 2003. Development of an efficient "substrate-trapping" mutant of Src homology phosphotyrosine phosphatase 2 and identification of the epidermal growth factor receptor, Gab1, and three other proteins as target substrates. J. Biol. Chem. **278**:13952–13958.
3. **Benezra R.** 1994. An intermolecular disulfide bond stabilizes E2A homodimers and is required for DNA binding at physiological temperatures. Cell **79**:1057–1067.
4. **Bennett AM, Hausdorff SF, O'Reilly AM, Freeman RM, Neel BG.** 1996. Multiple requirements for SHPTP2 in epidermal growth factor-mediated cell cycle progression. Mol. Cell. Biol. **16**:1189–1202.

5. **Chan G, Kalaitzidis D, Neel BG.** 2008. The tyrosine phosphatase Shp2 (PTPN11) in cancer. Cancer Metastasis Rev. **27**:179–192.
6. **Chen CY, Willard D, Rudolph J.** 2009. Redox regulation of SH2-domain-containing protein tyrosine phosphatases by two backdoor cysteines. Biochemistry **48**:1399–1409.
7. **Cunnick JM, Mei L, Doupnik CA, Wu J.** 2001. Phosphotyrosines 627 and 659 of Gab1 constitute a bisphosphoryl tyrosine-based activation motif (BTAM) conferring binding and activation of SHP2. J. Biol. Chem. **276**:24380–24387.
8. **Dance M, Montagner A, Salles JP, Yart A, Raynal P.** 2008. The molecular functions of Shp2 in the Ras/mitogen-activated protein kinase (ERK1/2) pathway. Cell. Signal. **20**:453–459.
9. **den Hertog J, Ostman A, Bohmer FD.** 2008. Protein tyrosine phosphatases: regulatory mechanisms. FEBS J. **275**:831–847.
10. **Dornan S, et al.** 2002. Differential association of CD45 isoforms with CD4 and CD8 regulates the actions of specific pools of p56lck tyrosine kinase in T cell antigen receptor signal transduction. J. Biol. Chem. **277**:1912–1918.
11. **Ferrari E, et al.** 2011. Identification of new substrates of the protein-tyrosine phosphatase PTP1B by Bayesian integration of proteome evidence. J. Biol. Chem. **286**:4173–4185.
12. **Finkel T.** 1998. Oxygen radicals and signaling. Curr. Opin. Cell Biol. **10**:248–253.
13. **Hanna N, et al.** 2006. Reduced phosphatase activity of SHP-2 in LEOPARD syndrome: consequences for PI3K binding on Gab1. FEBS Lett. **580**: 2477–2482.
14. **Hilpert K, Winkler DF, Hancock RE.** 2007. Peptide arrays on cellulose support: SPOT synthesis, a time and cost efficient method for synthesis of large numbers of peptides in a parallel and addressable fashion. Nat. Protoc. **2**:1333–1349.
15. **Hof P, Pluskey S, Dhe-Paganon S, Eck MJ, Shoelson SE.** 1998. Crystal structure of the tyrosine phosphatase SHP-2. Cell **92**:441–450.
16. **Hornbeck PV, Chabra I, Kornhauser JM, Skrzypek E, Zhang B.** 2004. PhosphoSite: a bioinformatics resource dedicated to physiological protein phosphorylation. Proteomics **4**:1551–1561.
17. **Huang Q, et al.** 2002. The novel role of the C-terminal region of SHP-2. Involvement of Gab1 and SHP-2 phosphatase activity in Elk-1 activation. J. Biol. Chem. **277**:29330–29341.
18. **Jorgensen C, et al.** 2009. Cell-specific information processing in segregating populations of Eph receptor ephrin-expressing cells. Science **326**: 1502–1509.
19. **Keilhack H, David FS, McGregor M, Cantley LC, Neel BG.** 2005. Diverse biochemical properties of Shp2 mutants. Implications for disease phenotypes. J. Biol. Chem. **280**:30984–30993.
20. **Kontaridis MI, Swanson KD, David FS, Barford D, Neel BG.** 2006. PTPN11 (Shp2) mutations in LEOPARD syndrome have dominant negative, not activating, effects. J. Biol. Chem. **281**:6785–6792.
21. **Lesage F, et al.** 1996. Dimerization of TWIK-1 K+ channel subunits via a disulfide bridge. EMBO J. **15**:6400–6407.
22. **Marin TM, et al.** 2011. Rapamycin reverses hypertrophic cardiomyopathy in a mouse model of LEOPARD syndrome-associated PTPN11 mutation. J. Clin. Invest. **121**:1026–1043.
23. **Martinelli S, et al.** 2008. Diverse driving forces underlie the invariant occurrence of the T42A, E139D, I282V and T468M SHP2 amino acid substitutions causing Noonan and LEOPARD syndromes. Hum. Mol. Genet. **17**:2018–2029.
24. **Matozaki T, Murata Y, Saito Y, Okazawa H, Ohnishi H.** 2009. Protein tyrosine phosphatase SHP-2: a proto-oncogene product that promotes Ras activation. Cancer Sci. **100**:1786–1793.
25. **Matozo HC, et al.** 2007. Low-resolution structure and fluorescence anisotropy analysis of protein tyrosine phosphatase eta catalytic domain. Biophys. J. **92**:4424–4432.
26. **Meng TC, Fukada T, Tonks NK.** 2002. Reversible oxidation and inactivation of protein tyrosine phosphatases in vivo. Mol. Cell **9**:387–399.
27. **Mesecke N, et al.** 2005. A disulfide relay system in the intermembrane space of mitochondria that mediates protein import. Cell **121**:1059–1069.
28. **Montagner A, et al.** 2005. A novel role for Gab1 and SHP2 in epidermal growth factor-induced Ras activation. J. Biol. Chem. **280**:5350–5360.
29. **Neel BG, Gu H, Pao L.** 2003. The 'Shp'ing news: SH2 domain-containing tyrosine phosphatases in cell signaling. Trends Biochem. Sci. **28**:284–293.
30. **Oishi K, et al.** 2009. Phosphatase-defective LEOPARD syndrome mutations in PTPN11 gene have gain-of-function effects during Drosophila development. Hum. Mol. Genet. **18**:193–201.
31. **O'Reilly AM, Pluskey S, Shoelson SE, Neel BG.** 2000. Activated mutants of SHP-2 preferentially induce elongation of Xenopus animal caps. Mol. Cell. Biol. **20**:299–311.
32. **Orton RJ, et al.** 2009. Computational modelling of cancerous mutations in the EGFR/ERK signalling pathway. BMC Syst. Biol. **3**:100.
33. **Ozawa T, Nakata K, Mizuno K, Yakura H.** 2007. Negative autoregulation of Src homology region 2-domain-containing phosphatase-1 in rat basophilic leukemia-2H3 cells. Int. Immunol. **19**:1049–1061.
34. **Rushworth LK, Hindley AD, O'Neill E, Kolch W.** 2006. Regulation and role of Raf-1/B-Raf heterodimerization. Mol. Cell. Biol. **26**:2262–2272.
35. **Saxton TM, et al.** 1997. Abnormal mesoderm patterning in mouse embryos mutant for the SH2 tyrosine phosphatase Shp-2. EMBO J. **16**:2352–2364.
36. **Scherz-Shouval R, et al.** 2007. Reactive oxygen species are essential for autophagy and specifically regulate the activity of Atg4. EMBO J. **26**:1749–1760.
37. **Shi ZQ, Lu W, Feng GS.** 1998. The Shp-2 tyrosine phosphatase has opposite effects in mediating the activation of extracellular signal-regulated and c-Jun NH_2-terminal mitogen-activated protein kinases. J. Biol. Chem. **273**:4904–4908.
38. **Shi ZQ, Yu DH, Park M, Marshall M, Feng GS.** 2000. Molecular mechanism for the Shp-2 tyrosine phosphatase function in promoting growth factor stimulation of Erk activity. Mol. Cell. Biol. **20**:1526–1536.
39. **Sugimoto S, Wandless TJ, Shoelson SE, Neel BG, Walsh CT.** 1994. Activation of the SH2-containing protein tyrosine phosphatase, SH-PTP2, by phosphotyrosine-containing peptides derived from insulin receptor substrate-1. J. Biol. Chem. **269**:13614–13622.
40. **Sundaresan M, Yu ZX, Ferrans VJ, Irani K, Finkel T.** 1995. Requirement for generation of H_2O_2 for platelet-derived growth factor signal transduction. Science **270**:296–299.
41. **Takada T, et al.** 1998. Roles of the complex formation of SHPS-1 with SHP-2 in insulin-stimulated mitogen-activated protein kinase activation. J. Biol. Chem. **273**:9234–9242.
42. **Tang TL, Freeman RM, Jr, O'Reilly AM, Neel BG, Sokol SY.** 1995. The SH2-containing protein-tyrosine phosphatase SH-PTP2 is required upstream of MAP kinase for early Xenopus development. Cell **80**:473–483.
43. **Tapia V, et al.** 2008. Evaluating the coupling efficiency of phosphorylated amino acids for SPOT synthesis. J. Pept. Sci. **14**:1309–1314.
44. **Tartaglia M, Gelb BD.** 2010. Disorders of dysregulated signal traffic through the RAS-MAPK pathway: phenotypic spectrum and molecular mechanisms. Ann. N. Y. Acad. Sci. **1214**:99–121.
45. **Tartaglia M, et al.** 2006. Diversity and functional consequences of germline and somatic PTPN11 mutations in human disease. Am. J. Hum. Genet. **78**:279–290.
46. **Tartaglia M, et al.** 2001. Mutations in PTPN11, encoding the protein tyrosine phosphatase SHP-2, cause Noonan syndrome. Nat. Genet. **29**: 465–468.
47. **Tartaglia M, et al.** 2003. Somatic mutations in PTPN11 in juvenile myelomonocytic leukemia, myelodysplastic syndromes and acute myeloid leukemia. Nat. Genet. **34**:148–150.
48. **Tertoolen LG, et al.** 2001. Dimerization of receptor protein-tyrosine phosphatase alpha in living cells. BMC Cell Biol. **2**:8.
49. **Voena C, et al.** 2007. The tyrosine phosphatase Shp2 interacts with NPM-ALK and regulates anaplastic lymphoma cell growth and migration. Cancer Res. **67**:4278–4286.
50. **Vogel W, Ullrich A.** 1996. Multiple in vivo phosphorylated tyrosine phosphatase SHP-2 engages binding to Grb2 via tyrosine 584. Cell Growth Differ. **7**:1589–1597.
51. **Wang N, et al.** 2006. Antagonism or synergism. Role of tyrosine phosphatases SHP-1 and SHP-2 in growth factor signaling. J. Biol. Chem. **281**: 21878–21883.
52. **You M, Yu DH, Feng GS.** 1999. Shp-2 tyrosine phosphatase functions as a negative regulator of the interferon-stimulated Jak/STAT pathway. Mol. Cell. Biol. **19**:2416–2424.